

Review of practical accuracies of geometrical sensor models of very high resolution satellite imagery

Luong Chinh Ke

Warsaw University of Technology
Institute of Photogrammetry and Cartography
1 Plac Politechniki, Warsaw, Poland
lchinhke@gazeta.pl

Received: 11 November 2006/Accepted: 23 February 2007

Abstract: Today, the new era with Very High Resolution Satellite (VHRS) imageries as IKONOS, QuickBird, EROS, OrbView etc., provides orthophoto in large scale of 1:5 000, to update existing maps, to compile general-purpose or thematic maps. Orthophotomap in the scale of 1:5 000 with Ground Sampling Distance of 0.5 m is one of three important sources for establishing GIS together with a Digital Elevation Model of ± 1.0 m accuracy in height and a topographic map in the scale of 1:10 000. Therefore, the accuracy of products of VHRS imageries affects reliability of GIS. Nevertheless, the accuracy of products of processing VHRS imageries is at first dependent on chosen geometrical sensor models. The understanding of geometrical sensor models of VHRS imageries is very important for improving processing of VHRS imageries.

The polynomial models are to provide a simple, generic set of equations to represent the indirect relationship between the ground and its image. The polynomial models or replacement sensor models must not only model the ground-to-image relationship accurately. Physical (or parametrical) model describes directly strict geometrical relations between the terrain and its image, using satellite's orbital parameters and basing on the co-linearity condition. In such model, the above-mentioned multi-source distorting factors are taken into consideration.

In this paper a review of practical accuracy of geometrical models of VHRS imageries taken from different research institutions in the world in last years has been presented.

Keywords: Very high resolution satellite imagery, orthorectification, ground sampling distance, physical and polynomial model, accuracy

1. Introduction

Since the beginning of 21th century, Very High Resolution Satellite (VHRS) imageries such as IKONOS, QuickBird, OrbView (USA), ALOS (Japan), EROS (Israel), SPOT-5 (France), KartoSat (IRS – India) etc., have been commercially used for different economical goals. In close time Pleiades imageries (France, 2009) with Ground Sampling Distance (GSD) equal to 0.71 m, WorldView, GeoEye imageries (USA, 2007) with GSD equal to 0.47 m and 0.41 m, respectively, and others commercial ones having

GSD lower than 0.5 m will appear on the world market. They create a new trend of utilization of super high resolution satellite (SHRS) imageries with $GSD \leq 0.5$ m for large scale mapping (1:5 000 – 1:2 000), generating orthophotomaps with a pixel of 0.5 m and DEM with height accuracy of 1.0 m. Those three products provide main, important sources of data for composing GIS. The reliability of GIS depends on the quality of those products that in row depends on chosen imageries geometrical models used in processing. The understanding of geometrical models of VHRS imageries is very important to improve the processing for generating DEM, orthophotomap and mapping. Geometrical models of VHRS imageries may be built on the basis of the relation between the terrain and its image at the exposure moment in satellite orbit. Geometrical models of VHRS imageries can be classified in two groups: a so-called parametrical (physical) or rigorous (strict) and polynomial or replacement models.

The purpose of a replacement model is to provide a simple, generic set of equations to accurately represent the ground-to-image relationship of the physical camera. A replacement model describes the ground-to-image relationship accurately. In the following sections, the RPC model and others of high resolution satellite that represented the indirect relation between the terrain and its image acquired on the flight orbit (Grodecki et al., 2004, 2003; Dial and Grodecki, 2003, 2004, 2005) will be described.

Physical (or parametrical) model describes directly strict geometrical relations between the terrain and its image basing on the co-linearity condition. In such model the above-mentioned multi-source distorting factors are taken into consideration. In the event of classical photogrammetric image, such strict model is based on the assumption of co-linearity, which is fundamental for photogrammetry. Condition of co-linearity is also fundamental for the construction of the strict model of satellite images. However, in this case it might be applied not to the entire image, but just to a single line. So, the elements of satellite image orientation cannot be discussed in a sense as it is in the case of aerial photographs. Values of orientation elements are a subject to continuous change, so the discussion will rather concern the function of those elements in relation to time. In literature one can find information on the construction of such models developed by different research centres. However, their authors do not disclose their final forms. Such models quite often include a lot of unknown elements – parameters, which values for a given image are determined on the basis of the Ground Control Points (GCPs) of known localization on the ground and identified on the image (Luong and Wolniewicz, 2005a, 2005b; Michalis and Dowman, 2003, 2005).

In last five years the investigations on geometrical models of VHRS imageries have been carried out in different research institutions in the world. The paper presents a review of accuracy analysis of chosen models of VHRS imageries that have been developed in world's known research centres.

2. Polynomial models

The purpose of polynomial (replacement camera) models is to provide a simple, generic set of equations for accurate representation of the ground-to-image relationship of the

physical camera. That relationship might be written as $(x, y) = F(X, Y, Z)$ where $F(\cdot)$ is the replacement camera model function, x, y are image coordinates, and X, Y, Z are respective ground coordinates (Fig. 1).

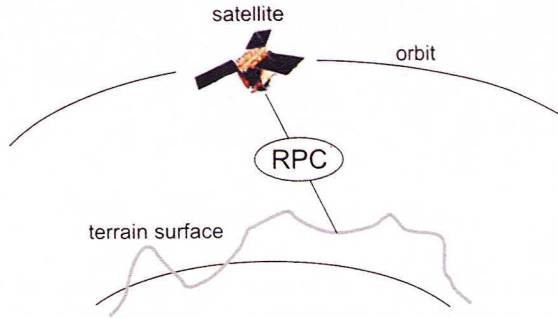


Fig. 1. The geometric relationship between imagery and Earth's surface described by RPC model

In practice, the Rational Polynomial Coefficients (RPC) model is a principal one for VHRS imageries. The RPC model could be modified into several simple ones.

2.1. RPC model

The Rational Polynomial Coefficients (RPC) model of camera of VHRS imagery is one of the very important replacement camera models that are quite often used in practice. The RPC model is defined as follows

$$x = \frac{R_1(X, Y, Z)}{R_2(X, Y, Z)} = \frac{\sum_{i=0}^{m1} \sum_{j=0}^{m2} \sum_{k=0}^{m3} a_{ijk} X^i Y^j Z^k}{\sum_{i=0}^{n1} \sum_{j=0}^{n2} \sum_{k=0}^{n3} b_{ijk} X^i Y^j Z^k}; \quad y = \frac{R_3(X, Y, Z)}{R_4(X, Y, Z)} = \frac{\sum_{i=0}^{m1} \sum_{j=0}^{m2} \sum_{k=0}^{m3} c_{ijk} X^i Y^j Z^k}{\sum_{i=0}^{n1} \sum_{j=0}^{n2} \sum_{k=0}^{n3} d_{ijk} X^i Y^j Z^k} \quad (1)$$

where x, y and X, Y, Z are the image and ground co-ordinates, respectively, and $a_{ijk}, b_{ijk}, c_{ijk}, d_{ijk}$ are the coefficients of polynomials.

The details on the RPC model can be found in (Dial and Grodecki, 2005; Grodecki et al., 2004). The practical accuracy of the RPC model for elaborating a single imagery and stereomodel is represented in Table 1 (Kaczynski and Ewiak, 2005; Nui et al., 2005).

Data in Table 1 indicates high accuracy of plane co-ordinate for single imagery obtained by the team of the Institute of Geodesy and Cartography (IGiK, Warsaw, Poland) headed by prof. Kaczynski, particularly for IKONOS imagery. Spatial co-ordinate accuracy for stereomodel obtained by researchers in Ohio University, Columbus, USA, depends on convergence angles of corresponding rays coming from left and right imagery.

Table 1. Accuracy of geometric correction of the VHRS single and stereo images base on the RPC model

Imageries	Single imagery				Stereomodel				
	GCP/ ICP*	m_x [m]	m_y [m]	IGiK (2005) Warsaw	GCP/ ICP	m_x [m]	m_y [m]	m_z [m]	Ohio University Convergence angles
IKONOS	5/26	0.39	0.39	Firm's RPC	4/6	1.14	1.06	1.29	Firm's RPC; 30.22°
QuickBird	7/24 11/24	0.78 0.31	1.00 0.30	Firm's RPC RPC with GCP	4/6	0.55	0.59	0.82	Firm's RPC; 61.64°

* GCP – Ground Control Points; ICP – Independent Check Points

2.2. Bias-compensated RPC model

VHRS imageries are the dynamic ones that became deformed with scale, shift and turn angle between scanning lines. Therefore, a correct RPC model has to be improved with those deformations. The new RPC model is a so-called bias-compensated RPC model or expanded RPC (ERPC) model

$$x = \frac{R_1(X, Y, Z)}{R_2(X, Y, Z)} - A_0 - A_1x - A_2y; \quad y = \frac{R_3(X, Y, Z)}{R_4(X, Y, Z)} - B_0 - B_1x - B_2y \quad (2)$$

where A_0, B_0 are the parameters describing the shifts in directions of x and y image's axes, A_1, B_1, A_2, B_2 are the parameters describing the scale change and turn angle.

Presentation of the ERPC model with its accuracy analysis for processing triplet and stereomodel of QuickBird and IKONOS imageries can be determined in the experiment (Hanley and Fraser, 2004). Table 2 presents the results.

Table 2. Spatial co-ordinate accuracies for triplet and stereomodel by the ERPC model

Imageries	GCP/ ICP	δ_0 [pixel]	Root Mean Square Error (RMSE)			Attention
			m_x [m/pixel]	m_y [m/pixel]	m_z [m/pixel]	
IKONOS	6/104	0.21	0.68/	0.26/	0.72/	Triplet
QuickBird	6/75	0.21	0.40/0.7	0.31/0.4	0.41/0.6	Stereo

Comparing data presented in Table 1 with those in Table 2 shows that the use of the ERPC model provides co-ordinates with higher accuracy than when using the RPC model.

2.3. Direct linear transformation

The relationship between terrain and its imagery can be expressed with a direct linear transformation (DLT). It is a particular case of the RPC model when the order of the polynomial in equation (1) equals to 1

$$\begin{aligned}x &= \frac{a_0 + a_1X + a_2Y + a_3Z}{1 + c_1X + c_2Y + c_3Z} \\y &= \frac{b_0 + b_1X + b_2Y + b_3Z}{1 + c_1X + c_2Y + c_3Z}\end{aligned}\quad (3)$$

where x, y and X, Y, Z are the image and ground co-ordinates, respectively, and a_i, b_i, c_i with $(i = 0, 1, 2, 3)$ are the coefficients of polynomials.

Uncertainty of the DLT model in terms of standard deviations is presented in Figure 2 (Jacobsen et al., 2005). It is clear that the errors of 2D coordinates of the DLT model are larger than those of other models.

2.4. Expanded direct linear transformation

Expanded direct linear transformation (EDLT) will be formed by expanding the direct linear transformation. It is defined as follows:

$$\begin{aligned}x &= \frac{a_0 + a_1X + a_2Y + a_3Z}{1 + c_1X + c_2Y + c_3Z} + a_4XY \\y &= \frac{b_0 + b_1X + b_2Y + b_3Z}{1 + c_1X + c_2Y + c_3Z} + b_4Y^2\end{aligned}\quad (4)$$

The parameters a_4, b_4 use to correct the errors of lateral and turn angle for $[XYZ]$ geodetic system with respect to imagery system $[xy]$. The accuracy of the EDLT model is better than the one of the DLT.

2.5. Affine transformation

The standard formula of the affine model is expressed as a transformation from 3D object space (X, Y, Z) to 2D imagery space (x, y)

$$\begin{aligned}x &= A_1X + A_2Y + A_3Z + A_4 \\y &= A_5X + A_6Y + A_7Z + A_8\end{aligned}\quad (5)$$

where $A_1 - A_8$ are the parameters of rotation, translation, non-uniform scaling and skew direction.

There are several motivations for using the affine model (Yamakawa and Fraser, 2004):

- the imaging planes are not parallel to each other; therefore, the affine model could experience accuracy degradation when employed in a Cartesian frame,
- the sensor's view direction with respect to Earth's ellipsoid normal does not change drastically since satellite's orbital ellipse for the imaging satellite has a focus at the centre of Earth's mass and has a small eccentricity; therefore, the constructed imagery planes retain near-parallelism in a map projection reference system,

- the combined effects of perturbed motion of sensor during image acquisition, the skew distortions caused by Earth's rotation and continuous changes of roll angle ω on the imagery.

Comparison of the errors of 2D coordinates of standard affine model (SAT) with those of other models is shown in Figure 2 (Jacobsen et al., 2005) and in Table 3 (Yamakawa and Fraser, 2004).

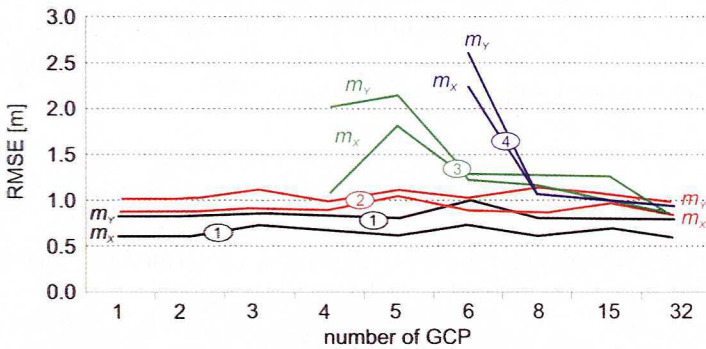


Fig. 2. The errors of 2D coordinates for ERPC (1), Hannover (2), SAT (3), and DLT (4) models

2.6. Dynamic affine transformation

It is known that VHRS imagery is a dynamic one. Each scanner line in the moment t has its own orientation elements. Standard affine transformation (SAT) must be expressed with the use of time-dependent functions. It means the coefficients in the equation (5) have to become functions of time t . This transformation is a so-called the dynamic-affine transformation (DAT)

$$\begin{aligned}
 x &= A_1(t)X + A_2(t)Y + A_3(t)Z + A_4(t) \\
 y &= A_5(t)X + A_6(t)Y + A_7(t)Z + A_8(t)
 \end{aligned}
 \tag{6}$$

where $A_1(t) - A_8(t)$ are time-variable (dynamic) parameters.

Estimated accuracy of the DAT model is expressed in Table 3 (Yamakawa and Fraser, 2004).

2.7. Expanded dynamic affine transformation

For correcting errors of scanner lines, the new terms of image values (x, y) in high power will be added to the equation (6). That way one acquires a new model of a so-called expanded dynamic-affine transformation (EDAT)

$$\begin{aligned} x &= A_1(t)X + A_2(t)Y + A_3(t)Z + A_4(t) + B_1x^2 + B_2y^2 \\ y &= A_5(t)X + A_6(t)Y + A_7(t)Z + A_8(t) + B_3x^2 + B_4y^2 \end{aligned} \quad (7)$$

where $B_1 - B_4$ are time-variable parameters.

The estimated accuracies of EDAT (7), DAT (6) and SAT (5) models are given in Table 3 (Yamakawa and Fraser, 2004).

Table 3. The estimated accuracies of SAT (5), DAT (6), and EADT (7) models

Single QuickBird			Stereo-QuickBird			Stereo-IKONOS				
Models	Left image σ_0 [pixel]	Right image σ_0 [pixel]	Number of GCP for model (7)	m_x [m]	m_y [m]	m_H [m]	Number of GCP for model (7)	m_x [m]	m_y [m]	m_H [m]
SAT (5)	10.40	15.95	15	0.50	0.48	0.60	9	0.62	0.43	0.73
DAT (6)	1.63	8.27	12	0.49	0.47	0.56	6	0.62	0.41	0.72
EDAT (7)	0.46	0.60	10	0.49	0.48	0.54	4	0.62	0.42	0.77

It is clear from Table 3 that the errors in X, Y, Z co-ordinates of the EADT model are smallest for single and stereomodel of QuickBird and IKONOS imagery. For QuickBird stereomodel the spatial co-ordinate accuracy can reach ± 0.5 m using 10 ground control points (GCP); for IKONOS, the spatial co-ordinate errors can reach ± 0.6 m using only 4 GCP.

2.8. Parallel projection model

It has been proven that the equation (5) is a particular case of parallel projection. However, it is well known that each scanner line is a central-perspective projection. Therefore, imagery co-ordinates based on central-perspective projection must be transformed into co-ordinates of parallel projection. It has also been proven that the suitable equation (5) based on parallel projection is (Morgan et. al., 2004; Zhang et al., 2004)

$$\begin{aligned} x &= A_1X + A_2Y + A_3Z + A_4 \\ y &= \frac{A_5X + A_6Y + A_7Z + A_8}{1 + (1/f)\tan(\psi)(A_5X + A_6Y + A_7Z + A_8)} \end{aligned} \quad (8)$$

where ψ is a lateral angle of scanner line. When $\psi = 0$, the equation (8) takes the form of (5).

Basing on the results of (Morgan et. al., 2004) presented in the Table 4, one can confirm that the accuracy of Z co-ordinates for parallel projection model (PP) (8) is better than for the SAT model (5).

Table 4. Accuracies for SAT (5) and PP (8) models

Standard deviation of ground coordinates	Accuracy estimation on GCP			Accuracy estimation on ICP		
	SAT model (5)	PP model (8) with using		SAT model (5)	PP model (8) with using	
		real value of Ψ	estimated value of Ψ		real value of Ψ	estimated value of Ψ
σ_{XY} [m]	1.675	<u>1.699</u>	1.685	1.666	<u>1.720</u>	1.690
σ_Z [m]	0.858	<u>0.070</u>	0.015	0.486	<u>0.039</u>	0.008

3. Parametrical models

Parametrical (or physical) model describes directly strict geometrical relations between the terrain and its image, basing on the co-linearity condition. In such model the above-mentioned multi-source distorting factors are taken into consideration.

In the moment t a satellite has position S and it performs scanner line in image system $(oxyz)$. Geometric relationship between image point q on image plane $(oxyz)$ and its terrain point Q in local ground system $OX_L Y_L Z_L$ is shown in Figure 3. This relation is connected with two systems: a so-called satellite system $SX_S Y_S Z_S$ and Earth's geocentric system $OXYZ$ (Luong and Wolniewicz, 2005a, 2005b). Models of co-linearity differ in terms of methods used to solve for parameters, including orbital ones, connecting an imagery with the terrain.

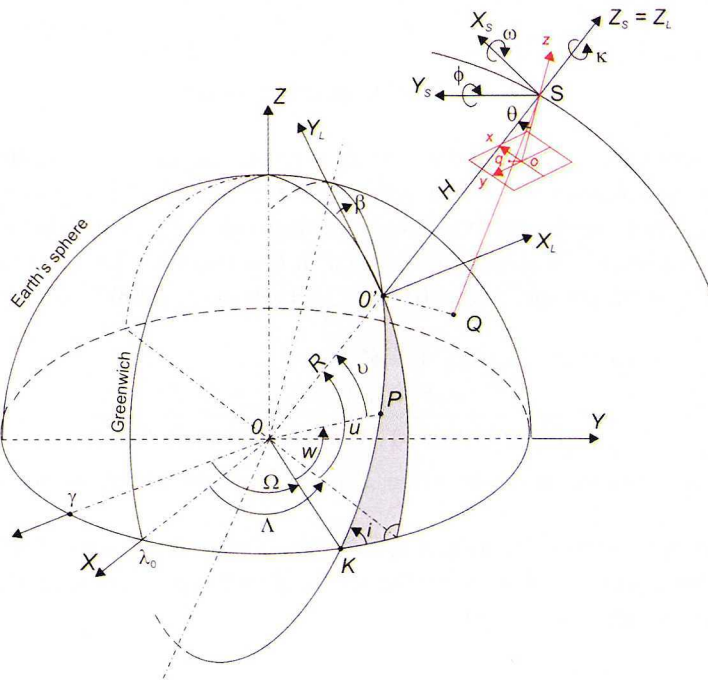


Fig. 3. Geometrical relationship between terrain and its imagery in the geocentric system $OXYZ$

3.1. Kepler model 1

Let X_L, Y_L, Z_L and X, Y, Z are the coordinates of the ground point Q in the local geodetic system $O'X_LY_LZ_L$ and the geocentric system $OXYZ$, respectively. Its corresponding position q on the image in the image system $oxyz$, taken from satellite S placed in elliptic orbit at a time epoch t is determined by spatial coordinates $x, y, -f$ (Fig. 3). The semi-major axis a and the eccentricity e are two metric parameters of satellite orbit, which define orbit's shape and size. Two angular parameters; orbit inclination i , and the longitude of ascending node Ω determine satellite orbit orientation in space. Finally, two other angular parameters: the argument of perigee w and true anomaly ϑ determine the position of a satellite in the orbit. Satellite position in a given orbit can be determined using polar coordinates: orbital radius r , where $r = OO' + O'S = R + H$ (R – Earth's mean radius, H – satellite altitude) and true anomaly ϑ . Let x_{ct}, y_{ct}, z_{ct} be the image point coordinates that were corrected with the errors of sensor's interior elements and of along-track inclination angle of sensor optical axis such as IKONOS, QuickBird, or cross-track angle as SPOT 1-4, IRS.

In Figure 3, γ denotes also vernal equinox, λ_0 – Greenwich meridian, K – ascending node, P – perigee, Λ – geocentric longitude, Φ – geocentric latitude.

Basing on the co-linearity condition there is the following relation

$$\begin{aligned} x_{ct} &= z_{ct} \frac{a_1(t)[X - X_S(t)] + a_2(t)[Y - Y_S(t)] + a_3(t)[Z - Z_S(t)]}{a_7(t)[X - X_S(t)] + a_8(t)[Y - Y_S(t)] + a_9(t)[Z - Z_S(t)]} \\ y_{ct} &= z_{ct} \frac{a_4(t)[X - X_S(t)] + a_5(t)[Y - Y_S(t)] + a_6(t)[Z - Z_S(t)]}{a_7(t)[X - X_S(t)] + a_8(t)[Y - Y_S(t)] + a_9(t)[Z - Z_S(t)]} \end{aligned} \quad (9)$$

where $a_i(t)$, ($i = 1, 2, 3, \dots, 9$) are the rotational matrix elements of a CCD array line that are functions of image exterior orientation elements ω, φ, κ and orbit angular parameters Ω, i, u ($u = w + \vartheta$) at epoch t ; $X_S(t), Y_S(t), Z_S(t)$ are coordinates of the perspective centre S at epoch t that are also the functions of satellite orbit parameters.

The equation (9) has thus a general form

$$\begin{aligned} F_{xt} \{x_{ct}, z_{ct}, X, Y, Z, \omega(t), \varphi(t), \kappa(t), i(t), \Omega(t), u(t), r(t)\} &= 0 \\ F_{yt} \{y_{ct}, z_{ct}, X, Y, Z, \omega(t), \varphi(t), \kappa(t), i(t), \Omega(t), u(t), r(t)\} &= 0 \end{aligned} \quad (10)$$

According to (10) each CCD array line is a function of 7 unknown parameters. IKONOS and QuickBird scenes consist of 3454 and 8656 lines, respectively. There is a large number of unknown parameters to be determined for one scene what practically makes impossible to obtain the solution.

In order to get the solution, the unknown parameters are considered as functions of time t or functions of CCD array lines l in the form of second order polynomial, i.e.

$$U_j(t) = \sum_{i=0}^2 c_{i,j} t^i \equiv \sum_{i=0}^2 d_{i,j} l^i \quad (11)$$

where $U(t)^T = [\omega(t), \varphi(t), \kappa(t), i(t), \Omega(t), u(t), r(t)]$ – the vector of unknown parameters, and $c_{i,j}, d_{i,j}$ are the coefficients to be determined.

First, the equation (10) will be transformed into observation equations, and then one can create the system of observation equations for three types of points, GCP, ICP and new points to be calculated (NCP).

Observation equation system is then converted into normal equation system that is further solved for unknown parameters. With the use of those parameters the transformation of coordinates of any image points into geocentric reference system, and next, into geodetic reference system will be performed.

It is necessary to remember that all GCP have to be, at the first step, transformed into the geocentric reference system, in which all operations will be done. The details concerning the solution of the presented model can be found in (Wolniewicz et al., 2005; Wolniewicz and Luong, 2006).

3.2. Kepler model 2

Satellite orbital parameters can be determined basing on given position vector and velocity vector of the satellite (satellite state vector) at the moment t . On the other hand, with given orbital parameters satellite's state vector can be calculated.

The model concerns a simple case when two imageries creating the stereomodel were acquired on along-track orbit. In Kepler model 2, six parameters of single imagery that determine satellite state vector at the moment t are three satellite position co-ordinates and its three velocity components in $SX_S Y_S Z_S$ system. Let (X_0, Y_0, Z_0) be a position vector of scanner line centre at $t = 0$ for first (left) imagery and (v_X, v_Y, v_Z) – a velocity vector of scanner line centre. The scanner line centre at the moment t for the imagery pair being a stereomodel will be a function of time t :

$$\begin{aligned} X_S(t) &= X_0 + v_x T - GM \frac{X_0}{2(X_0^2 + Y_0^2 + Z_0^2)^{3/2}} T^2 \\ Y_S(t) &= Y_0 + v_y T - GM \frac{Y_0}{2(X_0^2 + Y_0^2 + Z_0^2)^{3/2}} T^2 \\ Z_S(t) &= Z_0 + v_z T - GM \frac{Z_0}{2(X_0^2 + Y_0^2 + Z_0^2)^{3/2}} T^2 \end{aligned} \quad (12)$$

where $T = t$ for the first (left) imagery, $T = t + dt$ for the second (right) imagery, dt is time interval between the centres of begin scanner line for each image, $GM = 398600.4415 \text{ km}^3/\text{s}^2$ is Earth's gravitational coefficient.

The accuracy of Keplerian model 2 for SPOT-5 HRS Pan with GSD = 5 m, B/H = 0.8, using different variants of number of ground control points (GCP) such as 12 GCP, 6 GCP, 4 GCP, 3 GCP and 21 ground independent check points (ICP) is shown in Table 5 (Michalis and Dowman, 2004).

3.3. Lambert-Gauss model

Lambert-Gauss model is used only for a pair of imagery on along-track orbit creating a stereomodel. The co-ordinates of the centre of begin scanner line at moment t for the first (left) imagery $X_S^{(1)}(t), Y_S^{(1)}(t), Z_S^{(1)}(t)$ are (Michalis and Dowman, 2005):

$$\begin{aligned} X_S^{(1)}(t) &= X_1 + v_{1,x}t - \frac{1}{2}a_{1,x}t^2 = X_1 + \frac{X_2 - fX_1}{g}t - GM \frac{X_1}{2(X_1^2 + Y_1^2 + Z_1^2)^{3/2}}t^2 \\ Y_S^{(1)}(t) &= Y_1 + v_{1,y}t - \frac{1}{2}a_{1,y}t^2 = Y_1 + \frac{Y_2 - fY_1}{g}t - GM \frac{Y_1}{2(X_1^2 + Y_1^2 + Z_1^2)^{3/2}}t^2 \\ Z_S^{(1)}(t) &= Z_1 + v_{1,z}t - \frac{1}{2}a_{1,z}t^2 = Z_1 + \frac{Z_2 - fZ_1}{g}t - GM \frac{Z_1}{2(X_1^2 + Y_1^2 + Z_1^2)^{3/2}}t^2 \end{aligned} \quad (13a)$$

Analogically, for the second (right) imagery $X_S^{(2)}(t), Y_S^{(2)}(t), Z_S^{(2)}(t)$:

$$\begin{aligned} X_S^{(2)}(t) &= X_2 + v_{2,x}t - \frac{1}{2}a_{2,x}t^2 = X_2 + \frac{g'X_2 - X_1}{f'}t - GM \frac{X_2}{2(X_2^2 + Y_2^2 + Z_2^2)^{3/2}}t^2 \\ Y_S^{(2)}(t) &= Y_2 + v_{2,y}t - \frac{1}{2}a_{2,y}t^2 = Y_2 + \frac{g'Y_2 - Y_1}{f'}t - GM \frac{Y_2}{2(X_2^2 + Y_2^2 + Z_2^2)^{3/2}}t^2 \\ Z_S^{(2)}(t) &= Z_2 + v_{2,z}t - \frac{1}{2}a_{2,z}t^2 = Z_2 + \frac{g'Z_2 - Z_1}{f'}t - GM \frac{Z_2}{2(X_2^2 + Y_2^2 + Z_2^2)^{3/2}}t^2 \end{aligned} \quad (13b)$$

where (X_i, Y_i, Z_i) , $i = 1, 2$ are the co-ordinates of the centre of begin scanner line for first and second imagery at $t = 0$.

The accuracy of Lambert-Gauss model is presented in Table 5, using the same SPOT-5 imageries for the variant of 12 GCP and 21 ICP. It is clear that the accuracy of Lambert-Gauss model is the same as of Kepler model (Michalis and Dowman, 2004).

Table 5. Comparison between practical accuracies of parametrical models

RMSE [m]	Single image model		Kepler model 2					Lambert-Gauss model	
	12 GCPs	21 ICPs	12 ICPs	21 ICPs	6 GCPs 21 ICPs	4 GCPs 21 ICPs	3 GCPs 21 ICPs	12 GCPs	21 ICPs
m_x	5.80	12.18	5.72	11.10	12.21	12.57	13.27	5.69	11.99
m_y	7.25	18.90	9.46	10.76	13.78	19.93	26.36	9.65	11.36
m_z	6.35	11.33	5.79	9.86	12.58	13.34	16.37	5.88	11.53

3.4. Combined model

Combined model is written for three continuous imageries on along-track orbit (triplet). The velocity vector of scanner line centre for middle imagery $v_M = (v_{Mx}, v_{My}, v_{Mz})^T$ can be calculated as follows (Michalis and Dowman, 2005):

$$\begin{aligned}
 \mathbf{v}_M = & -dt_{2,M} \left(\frac{1}{dt_{M,1} \cdot dt_{3,1}} + \frac{GM}{12R_1^3} \right) \mathbf{R}_1 + \\
 & + (dt_{2,M} - dt_{M,1}) \left(\frac{1}{dt_{M,1} \cdot dt_{2,M}} + \frac{GM}{12R_M^3} \right) \mathbf{R}_M + \\
 & + dt_{M,1} \left(\frac{1}{dt_{2,M} \cdot dt_{2,1}} + \frac{GM}{12R_2^3} \right) \mathbf{R}_2
 \end{aligned} \tag{14}$$

where $\mathbf{R}_i = [X_i, Y_i, Z_i]^T$ with $i = 1, M, 2$ denotes geocentric vectors of centres of begin scanner lines for first (left), middle and second (right) imageries at $t = 0$.

Summary of parameter number for three parametrical models described above is shown in Table 6.

Table 6. Parametrical models with their parameters

Models		Parameters	Number of parameters				Formula for the number of parameters
			2 images	3 images	4 images	5 images	For N images
Single image model		$X_0, Y_0, Z_0, v_x, v_y, v_z, \varphi, \omega, \kappa$	18	27	36	45	$N(X_0, Y_0, Z_0, v_x, v_y, v_z) + N(\varphi, \omega, \kappa)$
Kepler model	1	$a, e, i, w, \Omega, \vartheta, \varphi, \omega, \kappa$	12	15	18	21	$(a, e, i, w, \Omega, \vartheta) + N(\varphi, \omega, \kappa)$
	2	$X_0, Y_0, Z_0, v_x, v_y, v_z, \varphi, \omega, \kappa$	12	15	18	21	$(X_0, Y_0, Z_0, v_x, v_y, v_z) + N(\varphi, \omega, \kappa)$
Lambert-Gauss model		$X_0, Y_0, Z_0, \varphi, \omega, \kappa$	12	-	-	-	$2(X_0, Y_0, Z_0) + 2(\varphi, \omega, \kappa)$
Combined model		$X_0, Y_0, Z_0, \varphi, \omega, \kappa$	-	18	24	30	$N(X_0, Y_0, Z_0) + N(\varphi, \omega, \kappa)$

Table 6 shows that single image model requires more parameters to be determined than the other ones. Both versions of Kepler model require least parameters. It means, Kepler models are very economical.

In the Institute of Photogrammetry and Cartography of the Warsaw University of Technology, Kepler models are further investigated.

4. Conclusions

In the new era Very High Resolution Satellite (VHRS) images as IKONOS, QuickBird, EROS, OrbView etc. with Ground Sampling Distance (GSD) even smaller than 1 m have been in potential for mapping, generating DEM and producing orthophotomap in large scale, to update existing maps, to compile general-purpose or thematic maps and for GIS.

The polynomial models are generic, simple models that do not require the given data of imaging sensor and orbit elements. Some advantages of polynomial models are simple implementation and no need for satellite orbit data and sensor calibration parameters, supporting any map projection system. Their disadvantages are the necessity of a large number of well distributed ground control points (GCP), impossibility to correct local distortion, the lack of physical interpretation of the model, decreased accuracy when image gets larger, and over parameterization and the dependency of the chosen polynomial on image and terrain characteristics. In practice, the RPC model is effectively used for orthorectifying IKONOS imageries of both flat and mountainous terrain with available accuracy up to ± 1.5 m. Using the coefficients of the RPC model supplied by image distributor, the minimum number of GCP, needed for orthorectification equals to 3. The RPC model can be used for QuickBird imagery of flat terrain with RMSE up to ± 1.5 m. With respect to VHRS imagery properties the other models such as ERPC, EDAT and PP have simple forms but have co-ordinates errors smaller than 1.0 m. Those models have been in the stage of studying.

The parametrical (physical) model based on co-linearity condition is a rigorous model. The advantages of a rigorous model of block triangulation are the possibilities to correct sensor distortion as well as other effects caused by Earth motion and map projection, to use time-dependent equation, orbital constraints and exterior orientation recorded by GPS/INS. The disadvantages of block adjustment are in difficulty to receive sensor physical parameters by vendor and in requiring specialized software for each sensor. In practice, using parametrical model the orthorectification accuracies of IKONOS and QuickBird are similar to each other with ground position errors from ± 1.0 m to ± 1.5 m. This model is suitable for QuickBird image of both flat and mountainous terrain. QuickBird image can be useful for generating orthophotomap in scale 1:5 000 with GSD of 0.5 m that is an essential information for GIS database.

In the Institute of Photogrammetry and Cartography of the Warsaw University of Technology, one continuously elaborates parametrical models for VHRS imagery that is presented in third section, basing on the physical-geometrical single image acquired in satellite orbit.

Acknowledgments

The author would like to thank Prof. S. Białousz of the Institute of Photogrammetry and Cartography, Warsaw University of Technology for helpful consultations and suggestions.

References

- Dial D., Grodecki J., (2003): *Block adjustment of high-resolution satellite images described rational function*, Photogrammetric Engineering and Remote Sensing, Vol. 69, No 1, pp. 59-68.
- Dial D., Grodecki J., (2004): *Satellite image block adjustment simulations with physical and RPC camera models*, ASPRS Annual Conference Proceedings, May 2004, Denver, Colorado (CD).

- Dial D., Grodecki J., (2005): *RPC replacement camera models*, International Archives of the Photogrammetry, Remote Sensing and Spatial Information Sciences, Vol. 34, part XXX.
- Dowman I., Michalis P., (2003): *Generic rigorous model for along track stereo satellite sensors*, ISPRS Workshop Proceedings, May 2003, Hannover (CD).
- Grodecki J., Dial D., Lutes J., (2003): *Error propagation in block adjustment of high-resolution satellite images*, ASPRS Annual Conference Proceedings, May 2003, Anchorage, Alaska (CD).
- Grodecki J., Dial D., Lutes J., (2004): *Mathematical model for 3D feature extraction from multiple satellite images described by RPCs*, ASPRS Annual Conference Proceedings, May 2004, Denver, Colorado (CD).
- Hanley H.B., Fraser C.S., (2004): *Sensor orientation for high-resolution satellite imagery: further insights into bias-compensated RPCs*, IAPRS of 20th Congress, Commission I, WG I/2, Istanbul (CD).
- Jacobsen K., Buyuksalih G., Topan H., (2005): *Geometric models for the orientation of high resolution optical satellite sensors*, ISPRS workshop proceedings of Commission I, WG I/5, May 2005, Hannover (CD).
- Kaczynski R., Ewiak I., (2005): *Correction IKONOS and QuickBird data for orthomaps generation*, 26th Asia Conference of Remote Sensing, Ha Noi (CD).
- Luong C.K., Wolniewicz W., (2005a): *Very high resolution satellite image triangulation*, 26th Asia Conference of Remote Sensing, Ha Noi (CD).
- Luong C.K., Wolniewicz W., (2005b): *Geometric models for satellite sensors*, Geodesy and Cartography, Polish Academy of Sciences, Vol. 54, No 4, pp. 191-203, Warsaw.
- Madami M., (2005): *Satellite image triangulation*, ISPRS workshop proceeding of Commission I, WG I/5, May 2005, Hannover (CD).
- Michalis P., Dowman I., (2004): *A rigorous model and DEM generation for SPOT5-HRS*, IAPRS of 20th Congress, Commission I, WG V/5, Istanbul (CD).
- Michalis P., Dowman I., (2005): *A model for along track stereo sensors using rigorous orbit mechanics*, ISPRS workshop proceedings of Commission I, WG I/5, May 2005, Hannover (CD).
- Morgan M., Kim K., Jeong S., Habib A., (2004): *Parallel projection modeling for linear array scanner scenes*, IAPRS of 20th Congress, Commission I, WG V/5, Istanbul (CD).
- Nui X., Zhou F., Di K., Li R., (2005): *3D geopositioning accuracy analysis based on integration of QuickBird and IKONOS imagery*, ISPRS workshop proceedings of Commission I, WG I/5, May 2005, Hannover (CD).
- Wolniewicz W., Kurczynski Z., Luong C.K., Kujawa L., Różycki S., (2005): *Geometric correction of very high resolution satellite images and their utilization for establishing topographic database* (in Polish), Research Project Nr 5T12E 00724, Institute of Photogrammetry and Cartography, Warsaw University of Technology, Poland.
- Wolniewicz W., Luong C.K., (2006): *Geometric modelling of VHRS Imagery*, ISPRS International Calibration and Orientation Workshop EuroCOW 2006, 25-27 January 2006, WG I/3, Castelldefels, Spain (www.isprs.org/commission1/uroCOW6).
- Yamakawa T., Fraser C.S., (2004): *The affine projection model for sensor orientation: experiences with high-resolution satellite imagery*, IAPRS of 20th Congress, Commission I, WG V/5, Istanbul (CD).
- Zhang J., Zhang Y., Cheng Y., (2004): *Block adjustment based on new strict geometric model of satellite images with high resolution*, IAPRS of 20th Congress, Commission I, WG V/5, Istanbul (CD).

Przegląd praktycznych dokładności geometrycznych modeli sensora dla wysokorozdzielczych obrazów satelitarnych

Luong Chinh Ke

Politechnika Warszawska
Instytut Fotogrametrii i Kartografii
Plac Politechniki 1, 00-661 Warszawa
e-mail: lchinhke@gazeta.pl

Streszczenie

Matematyczny opis zależności pomiędzy zdjęciem i terenem odgrywa ważną rolę w opracowaniu fotogrametrycznym, zwłaszcza dla wysokorozdzielczych obrazów satelitarnych. Obecnie, opracowanie wysokorozdzielczych obrazów satelitarnych dla tworzenia ortofotomap, generowania DEM/DTM jest zagadnieniem najczęściej opisywanym w literaturze. Budowa modeli sensora jest podstawą dla przetwarzania wysokorozdzielczych obrazów satelitarnych. W ostatnich latach, prace badawcze w wielu ośrodkach na świecie koncentrowały się na budowie modeli sensora.

Modele sensorów mogą być podzielone na dwie grupy: wielomianowe (lub zastępcze) i parametryczne (lub fizyczne). Modele wielomianowe opisują pośrednią zależność pomiędzy terenem i obrazem bez potrzeby znajomości parametrów orbity. Modele parametryczne opisują zaś bezpośrednią zależność pomiędzy terenem i obrazem przy użyciu parametrów orbity satelity.

W niniejszej pracy przedstawiono przegląd praktycznych dokładności modeli wysokorozdzielczych obrazów, zbadanych w ciągu ostatnich lat w różnych ośrodkach naukowo-badawczych.